

# Real-time Simulation of Cardiac Excitation Using Hardware-implemented Cardiac Excitation Modeling

Farhanahani Mahmud

Department of Electronic Engineering,  
Faculty of Electric and Electrical Engineering, Universiti Tun Hussein Onn Malaysia,  
86400 Parit Raja, Batu Pahat, Johor, MALAYSIA.

Received 1 October 2012; accepted 1 December 2012, available online 20 December 2012

**Abstract:** In this paper a hardware-implemented cardiac excitation model of a cardiac cell based on Luo-Rudy phase I (LR1) for the action potential (AP) generation in a mammalian cardiac ventricle is proposed to speed up the computational time during the simulation of the cardiac AP conduction. The hardware-implemented cardiac excitation model is designed by using analog circuits and a dsPIC microcontroller that could reproduce time-dependent and time-independent nonlinear current-voltage characteristics of six-type of ionic currents in LR1 model. Through the study, real-time simulations of reentrant excitation conduction of cardiac cells are realized by coupling 30 active circuits of the cell models based on a cable model. The real-time simulations of initiation have been performed by the model and they are comparable to those from the LR1 model. Thus, it is conceivable that the hardware-implemented cardiac excitation model may be useful as one of alternative tools toward further understanding of the reentrant mechanisms.

**Keywords:** Hardware-implemented cardiac excitation model, Luo-Rudy phase I model, reentrant

## 1. Introduction

In a normal heart, the electrical excitation wave dies when it reaches a complete activation of myocardium because of a refractoriness effect of the cardiac tissue that has excited before. Dysfunction of electrical excitation propagation could lead to unnatural contraction of cardiac muscle and preventing the heart to pump blood efficiently. Consequently it gives rise to arrhythmia which may lead to a rapid loss of consciousness or death. Under this uncommon condition, the propagating wave does not die out completely but re-excite the myocardium that has recovered from the refractoriness. In this case, excitation would rotate around an area of conduction block, which can be anatomically or functionally determined.

Most evident is reentry of cardiac excitation, which occurs when previously activated tissue is repeatedly activated by the propagating excitation wave as it reenters the same region and reactivates it at a frequency that is dependent on the velocity at which the wave-front conducts around the block, and the length of the path around the block. The most common type of reentry is circus movement reentry. For reentry to occur, whether anatomic or functional, unidirectional conduction block and the presence of excitable gap are essential. Unidirectional block occurs when a wave-front fails to propagate in one particular direction, but can continue to propagate in other directions. Generally, reentry can be understood through their mechanistic relationships to abnormal propagation.

Hence, to understand the electrophysiology of the heart, numerical cardiac models have been developed in order to simulate the electrical signals propagation of cardiac cells in variety of conditions. Somehow, this large scale of simulation requires an immense amount of computational time to run.

This paper reports our studies of constructing the hardware-implemented cardiac excitation model which includes analog circuits and a dsPIC microcontroller that could reproduce time-dependent and time-independent nonlinear current-voltage characteristics of the ionic channel currents in LR1 model. Moreover, an active circuit cable of the hardware-implemented cardiac excitation model is designed in a one dimensional closed ring to accomplish a real-time performance of reentrant action potential (AP) conduction and the mechanisms by which the reentrant wave is initiated and terminated are studied. The phase resetting phenomenon of the AP propagation which occurred during attempts at annihilating the reentrant wave is also analyzed. All of these simulations show comparable results to those that done by the numerical simulation of the LR1 model.

This paper is organized as follows. In Sec. 2, numerical model of Luo Rudy Phase I which is the base method in developing the hardware model is explained. In Sec. 3, details of the hardware-implemented cardiac excitation model of a cardiac cell are overviewed. In Sec. 4, details on a method of a cable model in performing the AP conduction are described. In Sec. 5, a manner and underlying mechanism in the initiation of the reentrant action conduction in a one dimensional ring shaped active circuit cable are discussed and compared with results

from the numerical simulation of the LR1 model. The initiation of the reentrant action conduction in a ring-shaped shown in two dimensional spatial contour mappings have also been presented for better understanding. Summary of the paper are lastly inferred in Sec.6.

## 2. Luo Rudy Phase I Model

Numerical models of cardiac cell are widely used in several studies related to the reentrant arrhythmia to investigate the underlying dynamics of reentrant wave [1-11]. Basically, these electrophysiology of isolated cardiac cell models are coupled together to perform simulations of action potential (AP) propagation in the cardiac tissue.

One of the models that have been used intensely in modeling the reentrant wave is Luo-Rudy phase 1 (LR1) model [1]. The LR1 model is a nonlinear ODE model of cardiac cell for the AP generation in a mammalian cardiac ventricle. It consists of eight time- and voltage-dependent variables and describes six-type ionic currents, the fast inward sodium current ( $I_{Na}$ ), the slow inward current ( $I_{si}$ ), the time-dependent potassium current ( $I_K$ ), the time-independent potassium current ( $I_{K1}$ ), the time-independent plateau potassium current ( $I_{kp}$ ) and the background current ( $I_b$ ) carried by sodium, potassium and calcium to represents the electrical properties of a cardiac cell.

As shown in Fig 1, LR1 model can be represented by an equivalent electrical circuit containing a capacitive component  $C_m$  representing the capacitance of the cell membrane per unit area, each of six resistive components with a voltage source representing a type of ion channel that allows an ionic current specific to each channel to influx and outflux the cell membrane.  $V_m$  is the membrane potential. These ionic currents are summed to give  $I_{ion}$  which represents the total current flowing through the ion channels (Eq. 1). Placing  $I_{ion}$  in parallel to the current through the capacitive component of the membrane circuit  $C_m$  yields the expression of Eq. 2 for the total current flow  $I_m$  through the membrane over time  $t$ .

$$I_{ion} = I_{Na} + I_{si} + I_K + I_{K1} + I_{kp} + I_b \quad (1)$$

$$I_m = C_m \frac{dV_m}{dt} + I_{ion} \quad (2)$$

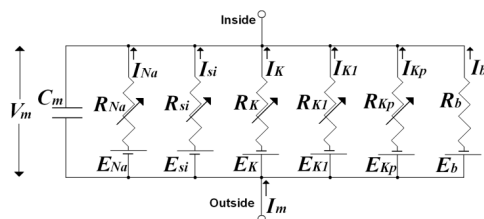


Fig. 1 An equivalent circuit representing membrane based on Luo-Rudy Phase I model.

Using this approach, it possible to exhibit reentrant waves in the form of one dimensional (1D), two dimensional (2D) or three dimensional (3D) and also may be able to identify specifically which components and mechanisms that are primarily responsible for the abnormal activity. Despite the conveniences, connecting large numbers of cell model units to form a simulation of cardiac excitation propagation requires plenty of computational time. In the current work, we have made an attempt to develop a hardware-implemented cardiac excitation model of a cardiac cell as a hardware adaptation of LR1 model that able to accomplish a real time simulation of the cardiac excitation propagation [12]. This hardware implementation may be useful as it is able to reduce the computational time during the simulation. Here, by using the model, we carried out a study on the mechanism reentrant arrhythmia in a one dimensional ring cable.

## 3. Hardware-implemented Cardiac Excitation Model of a Cardiac Cell

According to an equivalent circuit representing membrane based on LR1 model, the hardware-implemented cardiac excitation model is mainly presented as a parallel combination of a capacitance,  $C_m$  and the branches of analog circuit and a digital signal processor which correspond to the ionic currents in the LR1 model as illustrated in Fig. 2 and the action potential (AP) is produced by adding an external stimulus,  $I_{ext}$  (as  $I_m$ ) to the model.

It is known that in the LR1 numerical model, the amount of each ionic current depends on whether time-independent or time-dependent function of voltage,  $V_m$  and this relationship between voltage  $V_m$  and resulting ionic current can be considered as the current-voltage ( $I-V$ ) characteristic. Here, the hardware-implemented cardiac excitation model is constructed by applying electronic circuits to reproduce the  $I-V$  characteristic of all six-type ion channels. Analog circuits may suitable for ionic currents when they are constant or they change relative rapidly over time. Meantime, the digital implementations may be useful to represent ionic currents that change gradually over time.

In the study, the analog circuits were used to implement the time-independent ionic currents of  $I_{K1}$ ,  $I_{kp}$  and  $I_b$  and the time-dependent fast sodium current  $I_{Na}$  which has a relatively short time constant. Here, we designed analog circuits by exploiting the intrinsic voltage-current relationships of bipolar transistors ( $Tr$ ), resistors ( $R$ ), capacitors ( $C$ ) and voltage sources ( $V$ ) to reproduce the  $I-V$  characteristics. An electronic circuit simulation tool (Altium Designer version 6) was utilized to design the analog circuits. Meanwhile, for establishing a digital part of the model,  $I_K$  and  $I_{si}$ , were reproduced by using a 16-bit high-performance dsPIC30f4011 microcontroller with a processing speed near to 120MHz. The processing speed was thought to be considerable as initiatives have been taken to speed up the calculation process held by the dsPIC. To increase the speed of

calculation, we accessed certain data from constructed tables stored in the memory (ROM) rather than calculating the functions in equations which represent the ionic currents. Fig. 3 illustrates an overall circuit of the hardware-implemented cardiac excitation model where a circuit diagram of the digital part and a circuit diagram of the analog part are shown in Fig.4 and Fig.5, respectively. The analog circuits shown in panel A, B, C and D of Fig. 4 were constructed to reproduce the  $I-V$  characteristic of  $I_{K1}$ ,  $I_{Kp}$ ,  $I_b$  and  $I_{Na}$ , respectively. The hardware-implemented cardiac excitation model is actuated by direct current (DC) power supplies of 9V ( $V_+$ ) and -9V ( $V_-$ ).

By referring to Fig.3, the process of calculation in the hardware-implemented cardiac excitation model started with a voltage signal from the analog circuit corresponding to a cardiac cell membrane potential,  $V_m$  that was fed into a port of a 10-bit analog to digital converter of the dsPIC and was sampled with a frequency of 2.5kHz.  $I_K$  and  $I_{si}$  were calculated for each time instant and then an output voltage from the digital,  $V_{digital}$  corresponds to  $I_K$  and  $I_{si}$  were passed through a digital to 10-bit analog converter and were fed-back into the analog circuit. Next,  $V_{digital}$ ,  $V_m$  and an input of external impulsive signal,  $V_{pulse}$  were added and due to a potential difference which was set up within a resistor,  $R_7$ ,  $I_K$  and  $I_{si}$  from  $V_{digital}$ , and the external impulsive current,  $I_{pulse}$  from  $V_{pulse}$  flowed. Finally, they were added up with  $I_{Na}$ ,  $I_{K1}$ ,  $I_{Kp}$  and  $I_b$  from the analog circuit. The membrane potential,  $V_m$  changed through the current flow, and the quantity of charge stored in a capacitance,  $C_m$ , is equivalent to  $V_m$ .

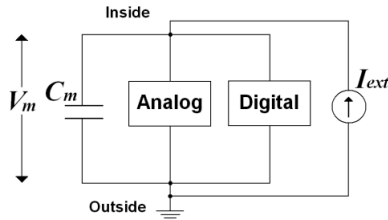


Fig. 2 A hardware-implemented cardiac excitation model. Ion currents were implemented by analog and digital circuits.

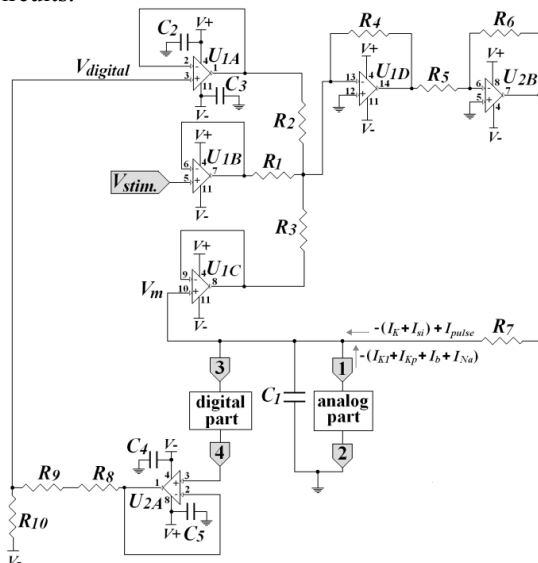


Fig. 3 An overall circuit of the hardware-implemented cardiac excitation model

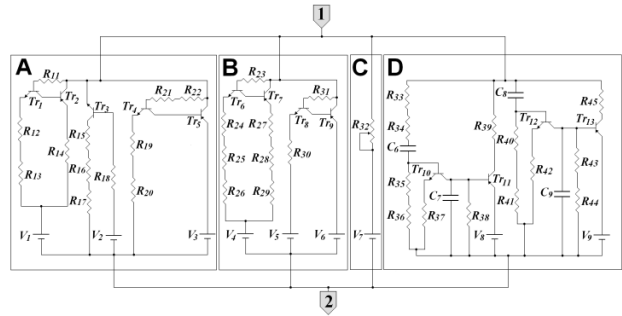


Fig. 4 A circuit diagram of an analog part in the hardware-implemented cardiac excitation model.

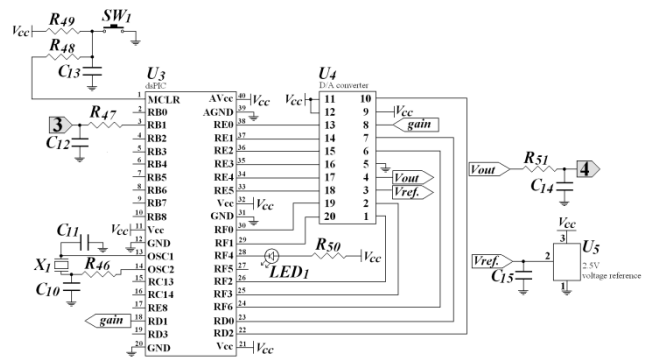


Fig. 5 A circuit diagram of a digital part in the hardware-implemented cardiac excitation model.

The time scale of the hardware-implemented cardiac excitation model was set to the same as the LR1 model. The current,  $I_{HM}$  and voltage scales,  $V_{HM}$  of the hardware-implemented cardiac excitation model (milli-Ampere and Volt) were not the same as those of the LR1 model (micro-Ampere and milli-Volt). The scale conversions of the voltage and the current were made because values of the ionic currents and the membrane potential in the LR1 model were too small and difficult to handle in the scale of the analog circuits. These values were converted as  $8\mu A$  to  $3mA$ ,  $-100mV$  to  $0V$  and  $120mV$  to  $5V$  (LR1 model to hardware-implemented cardiac excitation model). In formulae, the equations of the scales conversions of the voltage and the current were expressed in equation 3 and equation 4, respectively.

$$\frac{(V_{LR1} [mV] + 100)}{220} \cdot 5 \rightarrow V_{HM} [V] \quad (3)$$

$$I_{LR1} [\mu A] \cdot \left(\frac{3}{8}\right) \rightarrow I_{HM} [mA] \quad (4)$$

The AP waveform for a single membrane cell produced by the LR1 model is shown in the Fig. 10(a). The AP produced by the hardware-implemented cardiac excitation model is shown in Fig. 10(b). The AP in the panel (b) is converted to the scales of LR1 as shown in Fig. 10(c). In this case, an impulsive stimulation with a

duration time of 1 ms and an intensity of 80  $\mu\text{A}$  was applied to the models. By referring the panels (a) and (c) in Fig. 6, the AP waveform produced by the hardware-implemented cardiac excitation model was noted to be comparable to the waveform in the LR1 model as both models showed almost the same AP duration around 350 ms. Moreover, simulated AP patterns from the hardware-implemented cardiac excitation model in response to periodic current impulse trains with different interval were also comparable results with those from the LR1 model [12].

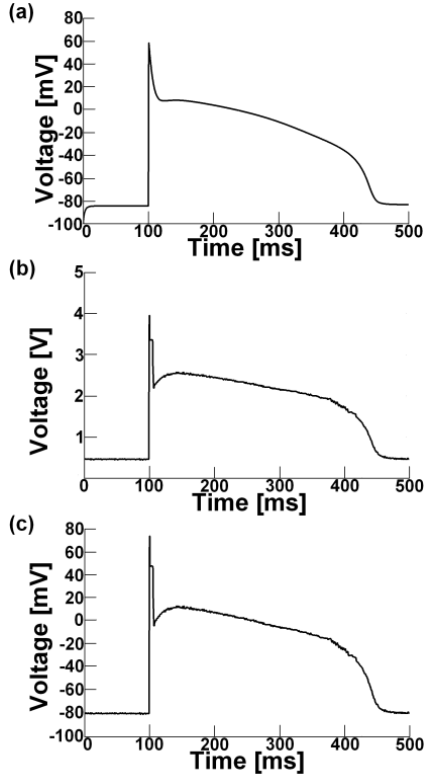


Fig. 6 Simulated action potential (AP) waveforms. Panels (a) and (b) represent the AP waveforms generated by the Luo-Rudy phase I model and the hardware-implemented cardiac excitation model, respectively. Panel (c) shows the AP waveform in the hardware-implemented cardiac excitation model after the scale conversion.

#### 4. An Active Circuit Cable Model

Cardiac cells are interconnected via gap junctions, thereby allowing propagation of these electrical excitations from cell to cell in tissue. The cardiac excitations propagate diffusively in tissue, therefore cardiac electrical behavior is governed by reaction-diffusion equation, also known as the cable equation. The simulation of excitation propagation in a one dimensional (1D) ring can be represented by a differential equation 5.

$$\frac{\partial V_m}{\partial t} = G(\Delta V_m) - \frac{I_{ion}}{C_m} \quad (5)$$

Where  $V_m$  is the cardiac cell membrane voltage,  $G$  is the conductivity tensor,  $C_m$  is the membrane capacitance, and  $I_{ion}$  is the ionic current specified by the cardiac cell

model formulation used where in this work, the  $I_{ion}$  is specified by LR1 model. According this equation, the cable model of the 1D ring consists of  $N$  cell models can be illustrated as a Fig. 7 where a gap junction resistance,  $R$  is corresponded to  $1/G$ . In this study, the cable model of the 1D ring was realized by coupling 30 cell models together with a gap junction resistance of  $R=2.35\text{k}\Omega$  which is equaled to  $1/G = 0.426\text{kS}$ . The applied value of  $R$  is considered relevant as it belongs in the range that provides a moderate coupling and allows a propagation of the action potential (AP).

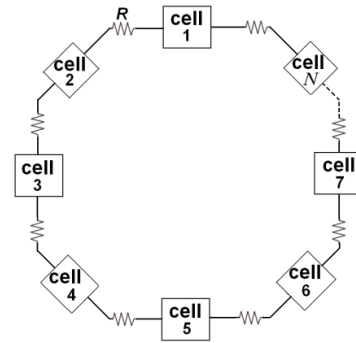


Fig. 7 A ring-shaped cable model. The ring model consists of  $N$  cell models and gap junction resistance,  $R$ .

#### 5. Reentrant Action Potential Conduction in a Ring-shaped Cable Model

In this project, a real-time simulation of an anatomical circus reentry around the closed ring active circuit cable consists of thirty the active circuits has been performed. The first stimulus (S1)-second stimulus (S2) protocol with a impulsive stimulation duration of 1ms and an intensity of  $150\mu\text{A}$  was applied to generate the action potential (AP) propagation where the S1 is used to pace at a fixed cycle length and the S2 is then applied at an initial interval after the S1. Basically, the stimulations need to be held twice to provoke the reentry, thus the S1-S2 protocol is appropriate as a pacing stimulus for generating the reentrant wave.

Here, as shown in Fig. 8, we constructed an impulsive stimulator by using an H8/3694F microcontroller to control the timing of the stimulation more effectively in realizing the phenomena of reentry. The device was powered by the same source with the digital part. To analyze the agreement between the hardware-implemented cardiac excitation model and the LR1 model, we also carried out numerical simulations of reentrant propagation in the 1D ring of the cable model by using the LR1 model. The simulations were made under the same conditions with those of the active circuit cable of the hardware-implemented cardiac excitation model.

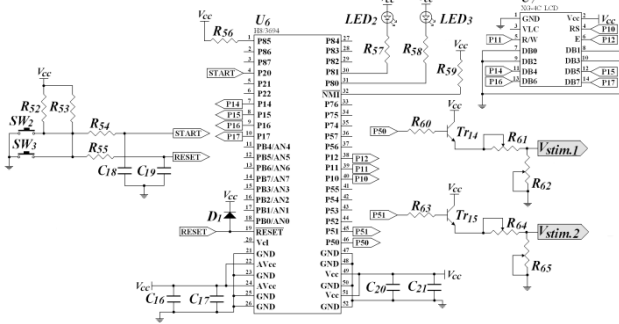


Fig.8 A circuit diagram of a impulsive stimulator.

Fig. 9 and Fig. 10 show a space-time diagram showing a change in membrane voltage during the initiation of circus movement reentry as a function of time and position around the ring presented by the hardware-implemented cardiac excitation model and by numerical model of the LR1, respectively. According to the figures, initially, the ring is stimulated at the number of cell,  $N = 1$  for 2 times. The first stimulus caused AP waves to propagate around both sides of the ring. These APs collide at the point opposite (in the ring state) the stimulation location, resulting in the annihilation of the AP waves. Following the second beat, an ectopic beat is being given at a position slightly offset from the original stimulation point, the number of cell,  $N = 5$ . The resulting excitation wave attempts to propagate in both directions around the ring, but one direction is refractory because of insufficient recovery from the previous excitation wave. As a result, the wave propagates in one direction and blocks in the other direction. After the excitation wave due to the second beat has annihilated, only the wave initiated with the third beat remains, thereby initiating circus movement reentry.

The contour mappings of AP waves represent the circus movement reentry around the closed ring hardware-implemented cable model is shown in Fig. 11, where the outer side of the mappings represent the spatial maps of the closed ring-shaped cable. Red and blue contour maps correspond to positive and negative values for the membrane potential. Here, red and blue contour maps correspond to positive and negative values for the membrane potential.

Fig. 11(1), which is at simulation time of 230ms, shows that the ring cable tissue model is in resting condition or has a negative value of membrane potential. According to the S1-S2 protocol for the reentrant initiation, then, S1 stimulus is applied at upper left edge of the mapping as shown in Fig. 11(2) at 234ms of the simulation time. This causes APs to propagate around both sides of the ring and they collide at the point on the ring opposite the stimulation site as shown in Fig. 11(3) to (10). By referring to Fig. 11(11), S2 stimulus is then applied at another spatial location of the upper side that results in an ectopic beat as in Fig. 11(12) to (14) and it propagate in one direction of anti-clock wise as the another direction is refractory because of insufficient recovery from the previous excitation wave initiated by the S1. This mechanism known as a unidirectional block

and it thereby initiating circus movement reentry as in Fig. 11(15) to (25) and beyond.

It is known that essential conditions for the initiation and maintenance of the reentry are the development of unidirectional block and the presence of an excitable gap within the front and back of the AP. It is known that LR model is a modification of the BR model, and the time constants of activation and inactivation of the slow inward calcium current in the BR model are unrealistically long [8]. Here, both models are modified by dividing time constants of activation and inactivation of the slow inward calcium current  $I_{si}$  with a factor of 12 to obtain the cycle length nearly 40ms and therefore enable the reentry in 30 cells of the ring cable model. By comparing these two figures, both models show the similar circumstances in the initiation of reentrant wave, although there is a small difference in the range of time between the S1 and S2 stimulus required for generating the reentrant wave. This may be due to small differences in the  $I-V$  characteristics between the LR1 model and the hardware-implemented cardiac excitation model, although the  $I-V$  characteristics of ionic channels in both models were noted to be generally comparable.

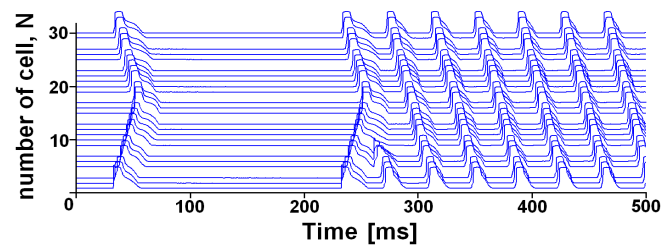


Fig. 9 A space-time diagram showing membrane voltage as a function of time and position around the ring-shaped cable presented by the hardware-implemented cardiac excitation active cable.

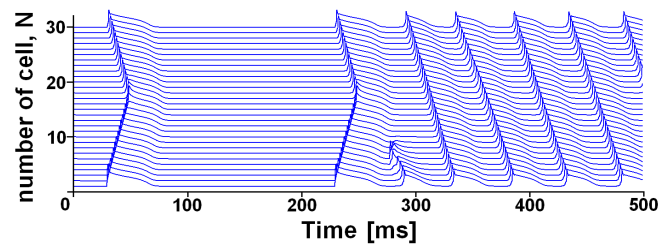


Fig. 10 A space-time diagram showing membrane voltage as a function of time and position around the ring-shaped cable presented by numerical model of the LR1.

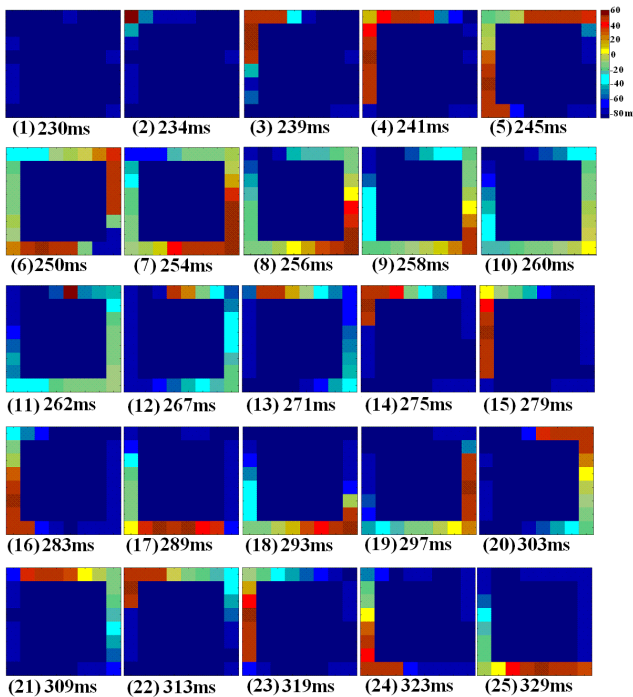


Fig. 11 Contour mappings of action potential (AP) waves during the circus movement reentry around the closed ring hardware-implemented cable model. Figure (1)-(25) show the reentry of APs in a sequential manner with the simulation time at 230ms to 329ms. Red and blue contour maps correspond to positive and negative values for the membrane potential.

## 6. Summary

In this paper, the hardware-implemented cardiac excitation model has been proposed which is capable to generate the action potential based on the Luo-Rudy phase I (LR1) model of a cardiac ventricular cell. The present hardware-implemented cardiac excitation model is able to carry out a real-time simulation of the excitation propagation in cardiac tissues. It is relevant to note that the increase number of the hardware-implemented cardiac excitation model will not reduce the speed, as each of them has its own computational time. In the study, we manage to perform the anatomical circus movement reentry in a one dimensional ring of the hardware-implemented cardiac excitation model cable. We analyzed phase resetting of the sustained reentry and also performed the simulation of reentrant wave termination. They generally correspond with the results from the LR1 model. From the result presented in the paper, we are concerned that the hardware-implemented cardiac excitation model could be one of alternative tools used in better understanding the mechanisms of reentry.

## Acknowledgement

This research is supported by the Short Term Grant funded by Universiti Tun Hussein Onn Malaysia (vote no. 0915), UTHM. The author gratefully acknowledges the support and advice of Professor Taishin Nomura, Osaka University.

## References

- [1] Luo C.H., Rudy Y., A model of the ventricular cardiac action potential, *Circ Res.* **68**, 1501-1526 (1991).
- [2] A. L. Hodgkin, A. F. Huxley, A quantitative description of membrane current and its application to conduction and excitation in nerve, *J. Physiol.* **117**, 500-544 (1952).
- [3] Beeler G. W., Reuter H., Reconstruction of the action potential of ventricular myocardial fibres, *J. Physiol.* **268**, 177-210 (1977).
- [4] Luo C.H., Rudy Y., A dynamic model of the cardiac ventricular action potential: I. simulations of ionic currents and concentration changes, *Circ Res.* **74**, 1071-1096 (1994a).
- [5] Nordin, Computer model of membrane current and intracellular  $Ca^{2+}$  flux in isolated in guinea pig ventricular myocyte, *Am j Physiol.* **265**, H2117-H2136 (1993).
- [6] Winslow RL, Rice J, Jafri S, marban E, O'Rourke B., Mechanisms of altered excitation-contraction coupling in canine tachycardia-induced heart failure, II: Model studies, *Circ Res.* **84**, 571-586 (1999).
- [7] Gregory M. Faber and Yoram Rudy, Action potential and contractility changes in  $[Na^+]_i$  overloaded cardiac myocytes: A simulation study, *Biophysical journal.* **78**, 2392-2404 (2000).
- [8] Aoxiang Xu, Micheal R. Guevara, Two forms of spiral-wave reentry in an ionic model of ischemic ventricular myocardium, *American Institute of Physics.* **8** (1), 157-172 (1998).
- [9] Taishin Nomura, Leon Glass, Entrainment and termination of reentrant wave propagation in a periodically stimulated ring of excitable media, *Physical Review E.* **53** (6), 6353-6360 (1996).
- [10] Marc Courtemanche, James P. Keener, Leon Glass, A delay equation representation of pulse circulation on a ring in excitable media, *SIAM J. Appl. Math.* **56**, 119-142 (1996).
- [11] A. Vinet, F. A. Roberge, The Dynamics of Sustained Reentry in a Ring Model of Cardiac Tissue, *Annals of Biomedical Engineering.* **22**, 568-591 (1994).
- [12] Mahmud F., Sakuhana T., Shiozawa N., Nomura T., An Analog-Digital Hybrid Model of Electrical Excitation in a Cardiac Ventricular Cell, *Trans. Jpn. Soc. Med. Biol. Eng.* **47** (5), 428-435 (2009).